# *A technique for error estimation of linewidth and damping parameters extracted from ferromagnetic resonance measurements*





| | |
|---|---|
| **Citation** | Buford, B., Dhagat, P., & Jander, A. (2015). A technique for error estimation of linewidth and damping parameters extracted from ferromagnetic resonance measurements. Journal of Applied Physics, 117(17), 17E109. doi:10.1063/1.4908301 |
| **DOI** | 10.1063/1.4908301 |
| **Publisher** | American Institute of Physics |
| **Version** | Version of Record |
| **Terms of Use** | http://cdss.library.oregonstate.edu/sa-termsofuse |

# A technique for error estimation of linewidth and damping parameters extracted from ferromagnetic resonance measurements

Benjamin Buford, Pallavi Dhagat, and Albrecht Jander[a)]
*School of Electrical Engineering and Computer Science, Oregon State University, Corvallis, Oregon 97331, USA*

(Presented 4 November 2014; received 23 September 2014; accepted 23 October 2014; published online 20 February 2015)

Ferromagnetic resonance (FMR) characterization, using a vector network analyzer (VNA), is widely used to determine anisotropy, g-factor, and Gilbert damping parameter of magnetic thin films, but results are typically reported without calculation of the measurement accuracy. We present a method of processing VNA-FMR measurements to determine both the value and confidence interval of these properties. The discussion is presented using FMR data obtained from stacks of MgO/CoFeB/Ta/CoFeB/MgO with varying CoFeB thickness. Measured S-parameters are de-embedded, drift corrected, fit to a Lorentzian curve, and analyzed to produce a confidence interval. A method of plotting the results of the Lorentzian fitting such that fitting errors or measurement drift can be visually analyzed is shown. © *2015 AIP Publishing LLC*. [http://dx.doi.org/10.1063/1.4908301]

## I. INTRODUCTION

Ferromagnetic resonance (FMR) spectroscopy is one of the most accurate and versatile methods of measuring magnetic material properties such as anisotropy, g-factor, and Gilbert damping parameter.[1,2] FMR characterization of damping in thin film magnetic materials has become critical for the growing magnetic random access memory (MRAM) industry.

While the anisotropy and g-factor can usually be obtained with good accuracy, the Gilbert damping parameter can be difficult to determine with precision due to low signal-to-noise ratios, particularly in ultra-thin films such as those constituting magnetic tunnel junction stacks. Yet, damping parameters are often reported in literature without comment on the goodness of the estimate of linewidth. In this work, we present a technique for analyzing FMR measurements, which includes quantifying the error in the damping parameter estimate. The discussion is presented using FMR data obtained from multi-layer stacks consisting of MgO/CoFeB/Ta/CoFeB/MgO with CoFeB in varying thicknesses.

The data analysis methods presented here are for fixed-frequency, swept field FMR measurements using a vector network analyzer (VNA) to measure the magnitude and phase of the four scattering parameters (S-parameters) of a broadband microwave waveguide loaded with the sample. It could also be applied, with minor modification, to fixed-field, swept frequency VNA-based measurements, but would not be applicable for FMR systems employing field-modulation and lock-in based measurements that do not record phase information.

## II. MEASUREMENT TECHNIQUE

The collection of data presented in this work is performed using a vector network analyzer to simultaneously measure the four S-parameters of a broadband coplanar waveguide loaded with a ferromagnetic thin film sample. Measurements are made at a fixed frequency while the magnetic field, applied perpendicular to the thin film sample, is swept 150 mT above and below the anticipated resonance point. The applied magnetic field is generated using a superconducting magnet and measured using a Hall effect sensor, as shown in Figure 1. At each programmed frequency, the magnetic field is ramped up and down ten times to collect multiple sweeps.

## III. DE-EMBEDDING

The loading of the waveguide with the sample film produces only a small perturbation of the S-parameters of the waveguide and cables. To isolate the absorption of the magnetic film alone, the field and frequency dependent S-parameters of the cabling and waveguide loaded with a bare substrate are measured prior to sample measurement.

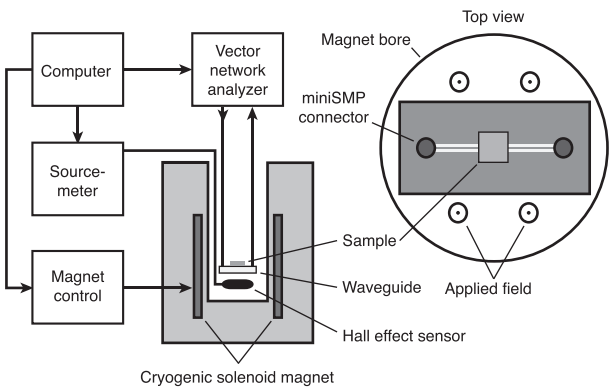


FIG. 1. Schematic of a cross section and top view of the measurement system. The waveguide and sample are placed in the bore of a Cryogenic Limited superconducting magnet, which creates a magnetic field out of the plane of the sample. The magnetic field is monitored using a Hall effect sensor and Keithley 2440 Sourcemeter. An Agilent E5224A PNA is used to measure the S-parameters of the coplanar waveguide.

[a)]Electronic mail: jander@eecs.oregonstate.edu.

 

A comparison of the S21 magnitude between a typical background measurement and the additional effect of a magnetic film is shown in Figures 2(a) and 2(b). The origin of the magnetic field dependence of the background measurement is unclear, but may be due to electron paramagnetic resonance in the waveguide and cabling, or ferromagnetic contamination.

S-parameter measurements are made asynchronously to the magnetic field sweep. Therefore, each field sweep is sampled at slightly different magnetic field values. To allow direct comparison between background and sample measurements, each background measurement field sweep is resampled to match all field values at which the thin film sample was measured. This is accomplished using kernel regression[3] with bandwidth and regularization parameter tuned independently per sweep. Once each background sweep has been resampled, all field sweeps for a given frequency are averaged. This process is repeated for each of the four measured S-parameters.

In prior work, various approaches have been employed to accomplish the de-embedding: simply fitting to measured S21 data,[4] dividing the measured S21 parameter by that of the background measurement,[5,6] or assuming a fixed phase shift and reflections due to imprecise sample placement.[7] These approximations work well for samples with large signals and low distortion from waveguide non-idealities. However, at certain frequency points, when the background measurement has significant magnetic field dependencies, we have found these approaches to produce erroneous results. Instead, we established a more complete de-embedding approach, which takes advantage of all four measured S-parameters of the background

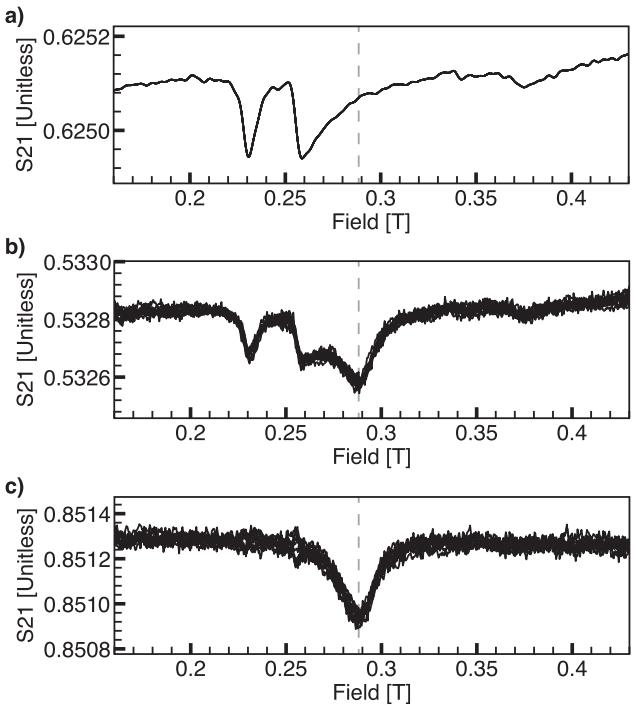


FIG. 2. A comparison of measured |S21| of a bare substrate after resampling and smoothing (a), substrate with a MgO/CoFeB (0.9 nm)/Ta/CoFeB (0.9 nm)/MgO stack (b), and results after de-embedding (c). Measurements were taken with a 19 GHz excitation.

to construct a nearly symmetric model of the waveguide. We assume the contribution of the thin film sample to the measured S-parameters occurs at a point in the middle of the waveguide. Thus, when the measured S-parameters are converted to scattering transfer parameters (T-parameters), they can be written in terms of the contribution of the sample as

$$[T_{meas}] = [T_a][T_{sample}][T_b], \tag{1}$$

where $[T_{meas}]$ is the measured T-parameter matrix, $[T_a]$ and $[T_b]$ are the T-parameter matrices of each half of the waveguide and cabling (corresponding to S-parameter matrices $[S_a]$ and $[S_b]$), and $[T_{sample}]$ is the T-parameter matrix of the sample alone. The background measurement $[T_{bg}]$ is then

$$[T_{bg}] = [T_a][T_b] = \begin{bmatrix} T11_a & T12_a \\ T21_a & T22_a \end{bmatrix}\begin{bmatrix} T11_b & T12_b \\ T21_b & T22_b \end{bmatrix}. \tag{2}$$

Typically, when de-embedding, each half of the fixture is characterized independently by splitting the fixture apart and attaching known loads. In this application, it is not practical to characterize half of the waveguide, so additional assumptions are required. If we assume, based on symmetry of the fixture, that $S12_a = S12_b$ and $S21_a = S21_b$, values for both $S_a$ and $S_b$ can be determined from the background S-parameters as

$$S22_a = \frac{S11 - S22\sqrt{S12\,S21}}{S12\,S21 - 1}, \tag{3}$$

$$S11_b = \frac{S22 - S11\sqrt{S21\,S12}}{S21\,S12 - 1}, \tag{4}$$

$$S11_a = S11 - S11_b\sqrt{S12\,S21}, \tag{5}$$

$$S22_b = S22 - S22_a\sqrt{S21\,S11}, \tag{6}$$

$$S12_a = S12_b = \sqrt{S12(1 - S22_a\,S11_b)}, \tag{7}$$

$$S21_a = S21_b = \sqrt{S21(1 - S22_a\,S11_b)}. \tag{8}$$

The T-parameters of the sample alone can then be calculated by left and right multiplying (1) by the inverse matrices $[T_a]^{-1}$ and $[T_b]^{-1}$. This de-embedding approach significantly decreases the false resonance peaks associated with the waveguide, as seen in Figure 2(c).

While both this de-embedding approach and the simpler approach of directly dividing the sample response from the background produce absorption curves which appear similar, the linewidth measurement is extremely sensitive to the curve shape. As such, our approach decreased the average variance in measured linewidth by up to 40% when compared to directly dividing the sample response from the background for our samples. It should be noted that this improvement only occurs at select frequency points, where reflections and waveguide resonances interfere with the sample resonance; in cases where the waveguide is well behaved, both approaches generate results and variances thereof within 5% variation.

## IV. LORENTZIAN FITTING

The de-embedded S-parameters for the sample are fitted to the susceptibility derived from the Landau-Lifshitz

equation.[6,8] As we are not interested in the absolute amplitude of absorption, only the resonance field and linewidth, we ignore the effects of the reflection terms (S11 and S22) when fitting. To allow for measurement drift, we include an arbitrary linear offset for each sweep, giving the equation

$$S21 = a + bH + \frac{c(H - M_{eff})M_{eff}}{(H - M_{eff})^2 - H_{eff}^2 \pm i\frac{\Delta H}{2}(H - M_{eff})}, \tag{9}$$

where $a$, $b$, and $c$ are complex-valued drift and amplitude fitting terms; $H$ is the applied field; $\Delta H$ is the full-width-half-maximum linewidth; $M_{eff} = M_s - H_k^{\perp}$, where $M_s$ is the saturation magnetization and $H_k^{\perp}$ is the perpendicular anisotropy field; $H_{eff} = 2\pi f/\gamma\mu_0$; $f$ is the frequency; $\mu_0$ is the permeability of free space; and $\gamma$ is the gyromagnetic ratio, is defined as $\gamma = g\mu_B/\hbar$. The values for $a$, $b$, and $c$ are fit separately for each field sweep, while $\Delta H$, $M_{eff}$, and $g$ are assumed constant across all sweeps at a given frequency. Figure 3 shows S21 and the best Lorentzian fit after the complex-valued drift and amplitude fitting terms have been estimated and removed (by subtracting $(a + bH)$ from (9) and then dividing by $c$).

Next, the resonance field as a function of frequency, $H_{res}$, is determined from the best fit values of $H_{eff}$ and $M_{eff}$ from each sweep

$$H_{res} = M_{eff} + H_{eff} = M_{eff} + \frac{f}{g}\frac{2\pi\hbar}{\mu_B\mu_0}, \tag{10}$$

and linear regression is used to estimate the value of $M_{eff}$. Since $M_{eff}$ can be assumed constant over frequency, a second iteration of fitting of the de-embedded data to (9) is performed with $M_{eff}$ held constant.

The linewidth estimates resulting from the Lorentzian fitting at different frequencies are then used to estimate the damping parameter, $\alpha$, by fitting the function

$$\Delta H = \frac{4\pi\alpha f}{|\gamma|\mu_0} + \Delta H_0, \tag{11}$$

where the first term is the damping contribution to the linewidth and $\Delta H_0$ is the inhomogeneous broadening.[9]

## V. ERROR ESTIMATION

As the measured value of $\Delta H$, and thus $\alpha$, is very susceptible to error from low signal-to-noise ratio, there is need to quantify the error in linewidth measurement in order to accurately calculate $\alpha$. When fitting the data to a Lorentzian curve with arbitrary amplitude, there is a strong correlation between $\Delta H$ and $c$, the amplitude fitting term, due to them both contributing to the amplitude of the curve at resonance. Due to this correlation, and the lack of knowledge of the linewidth error distribution, an examination of the covariance matrix of fitting parameters obtained from the least squares estimation fails to accurately capture the variance in linewidth alone; it produces variance values far in excess of the measured linewidth.

Instead, we are mainly interested in the relative quality of de-embedding and signal-to-noise ratio of each linewidth estimate for use in weighting during subsequent linear regression. To obtain this, we simplify the error analysis by considering a parametric plot of real and imaginary parts of the S21 values of a particular frequency measurement (after correcting for amplitude and offset drift) on the complex plane with magnetic field as the parameter, as shown in Figure 4. Ideally, this should produce a circle, which approaches the origin at field values far away from the resonance point and has a radius equal to $|M_{eff}|/\Delta H$. Assuming that $M_{eff}$ can be measured with precision, the radial distance of each data point to the best-fit circle represents the error in the linewidth estimate contributed by that point.

This plot provides a method to visualize errors in de-embedding and drift correction, as well as variance in the linewidth measurement. Poorly de-embedded signals may include secondary circles associated with resonances in the waveguide or cabling. Drift in the measurement will appear as either an offset from the origin, or a circle which does not

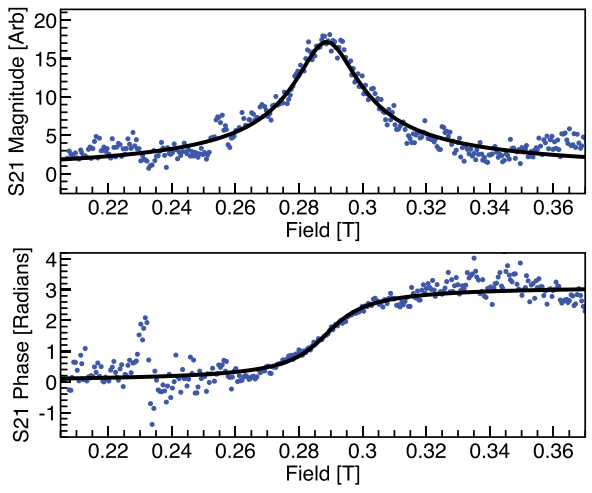


FIG. 3. Results of Lorentzian fitting of a single sweep after drift and amplitude terms are removed.

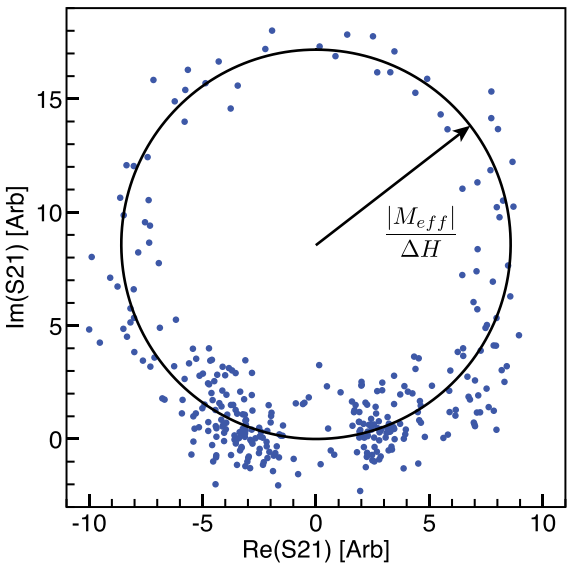


FIG. 4. Results of Lorentzian fitting (Figure 3) plotted on a complex plane; the result is a circle intersecting the origin with a radius of $|M_{eff}|/\Delta H$.

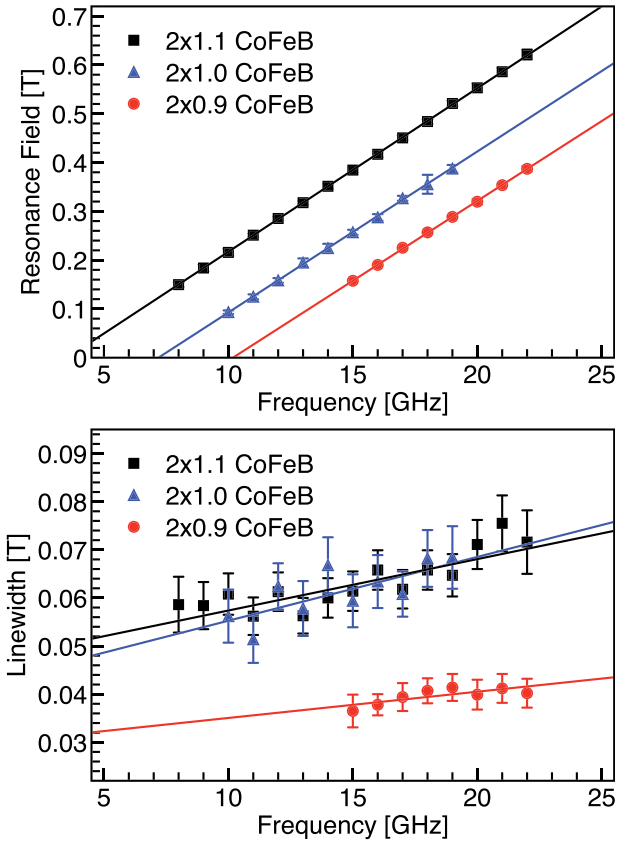


FIG. 5. Measured FMR linewidth and resonance field with 95% confidence intervals for samples presented in Table I.

close on itself. A low variance linewidth measurement will have all points clustered near the circle.

The residuals of $\Delta H$ can be calculated by finding the distance of each point on the circle to the center (located at $-M_{eff}/\Delta H$), and correcting for $M_{eff}$. As $M_{eff}$ can usually be accurately determined from the y-intercept of (10), the effects of the variance of $M_{eff}$ are ignored. For field sweep $m$, the standard deviation of linewidth, $\sigma_{\Delta H_m}$ can then be calculated by

$$\sigma_{\Delta H_m} = \sqrt{\frac{1}{N-1}\sum_{n=1}^{N}\left(\frac{M_{eff}}{\left|S21_{(m,n)} + i\frac{M_{eff}}{\Delta H_m}\right|} - \Delta H_m\right)^2}, \quad (12)$$

where $N$ is the number of sample points per field sweep. This process is repeated individually for each field sweep. Least-squares estimation[10] is used to fit the collection of sweep linewidth vs. frequency data to (11) using each sweep as a single datapoint with the corresponding calculated variance. This allows for estimation of $\alpha$ and its variance, $\sigma_\alpha^2$. The entire Lorentzian fitting and error estimation process can then be repeated using S12 (instead of S21) and the results combined to increase confidence.

TABLE I. Measured FMR parameters.

| CoFeB thickness (nm) | $g$ | $\mu_0 M_{eff}$ (mT) | $\alpha$ |
|---|---|---|---|
| $2 \times 1.1$ | 2.130 | −118 | $0.0159 \pm 0.0045$ |
| $2 \times 1.0$ | 2.168 | −237 | $0.0201 \pm 0.0093$ |
| $2 \times 0.9$ | 2.183 | −333 | $0.0083 \pm 0.0068$ |

Results of this fitting approach for a multi-layer stack of MgO/CoFeB/Ta/CoFeB/MgO with CoFeB thicknesses of 0.9 nm, 1.0 nm, and 1.1 nm are shown in Figure 5 and Table I. The error bars shown are the 95% confidence interval calculated by combining the linewidth variance for all field sweeps at each frequency point.

## VI. CONCLUSION

We constructed a method of post-processing ferromagnetic resonance measurements from a vector network analyzer in order to extract both the damping parameter and the confidence interval thereof. Our de-embedding approach decreases the variance in linewidth estimation by up to 40% when compared to simply dividing the sample measurement by background for select resonance fields. A method of visualizing the quality of de-embedding and drift correction is presented, and results for magnetic thin films of various thicknesses are shown. This approach allows for characterization of thin-film samples that exhibit very low signal-to-noise ratios by including a goodness-of-fit metric, which will become increasingly important in the future as thinner films are developed.

## ACKNOWLEDGMENTS

The authors thank Dr. Raviv Raich of Oregon State University for insight on the resampling methods used. This work was supported in part by a Grant from the Semiconductor Research Corporation.

[1]M. Farle, Rep. Prog. Phys. **61**, 755 (1998).
[2]I. Neudecker, G. Woltersdorf, B. Heinrich, T. Okuno, G. Gubbiotti, and C. H. Back, J. Magn. Magn. Mater. **307**, 148 (2006).
[3]T. Hastie, R. Tibshirani, and J. Friedman, *The Elements of Statistical Learning* (Springer, 2001), pp. 165–192.
[4]B. K. Kuanr, R. Camley, and Z. Celinski, J. Magn. Magn. Mater. **286**, 276 (2005).
[5]S. S. Kalarickal, P. Krivosik, M. Wu, C. E. Patton, M. L. Schneider, P. Kabos, T. J. Silva, and J. P. Nibarger, J. Appl. Phys. **99**, 093909 (2006).
[6]H. T. Nembach, T. J. Silva, J. M. Shaw, M. L. Schneider, M. J. Carey, S. Maat, and J. R. Childress, Phys. Rev. B **84**, 054424 (2011).
[7]C. Bilzer, T. Devolder, P. Crozat, C. Chappert, S. Cardoso, and P. P. Freitas, J. Appl. Phys. **101**, 074505 (2007).
[8]Y. Ding, T. J. Klemmer, and T. M. Crawford, J. Appl. Phys. **96**, 2969 (2004).
[9]J.-M. Beaujour, D. Ravelosona, I. Tudosa, E. E. Fullerton, and a. D. Kent, Phys. Rev. B **80**, 180415 (2009).
[10]D. York, N. M. Evensen, M. L. Martnez, and J. De Basabe Delgado, Am. J. Phys. **72**, 367 (2004).